Martín-García, N.; Vennestrom, PNR.; Thogersen, JR.; Moliner Marin, M.; Corma Canós, A. (2017). Iron-Containing SSZ-39 (AEI) Zeolite: An Active and Stable High-Temperature NH3-SCR Catalyst. ChemCatChem. 9(10):1754-1757. doi:10.1002/cctc.201601627

Iron-containing SSZ-39 (AEI) zeolite: an active and stable high temperature NH_3-SCR catalyst

Nuria Martín,[1] Peter N. R. Vennestrøm,[2] Joakim R. Thøgersen,[2] Manuel Moliner,[1]* Avelino Corma[1]*

[1] Instituto de Tecnología Química, Universitat Politècnica de València-Consejo Superior de Investigaciones Científicas, Avenida de los Naranjos s/n, 46022 Valencia, España

[2] Haldor Topsøe A/S, Haldor Topsøes Allé 1, DK-2800 Lyngby, Denmark

*Corresponding authors: E-mail addresses: acorma@itq.upv.es; mmoliner@itq.upv.es

Selective catalytic reduction of nitrogen oxides (NO_x = NO and NO_2) with ammonia (NH_3-SCR) has become one of the most effective methods used for treating exhaust gases from diesel vehicles and stationary sources (i.e. power plants).[1] Vanadia supported on titania (V_2O_5/TiO_2) has been widely applied and investigated as NH_3-SCR catalysts for both mobile and stationary applications.[2] However, vanadium based catalysts suffer from limited hydrothermal stability when treated at high reaction temperatures (e.g. above 650˚C). Alternative catalysts are based on transition metal containing zeolites.[3] Especially, copper-containing zeolites have shown to provide increased hydrothermal stability as well as high activity at low and medium temperatures, e.g. between 200 and 450ºC, that are typically achieved in the exhaust from vehicular internal combustion engines.[3,4]

In contrast, the abatement of NO_x from stationary sources, such as power plants and gas turbines, requires stable, active and selective catalysts at higher temperatures (>450ºC).[5] Unfortunately, copper-based zeolites show limited selectivity at higher temperatures due to unselective ammonia oxidation.[4] Iron-containing medium and large pore zeolites have been reported as convenient catalysts for NH_3-SCR at high reaction temperatures (>450ºC).[6] Nevertheless, these materials in general show insufficient hydrothermal stability at temperatures above 600ºC, due to the oligomerization of iron species.[6a]

In the last years, it has been reported that metal-containing small pore zeolites show higher hydrothermal stability compared to large or medium pore zeolites.[4,7] Particularly, iron-exchanged small pore chabazite (CHA) has been reported to be a hydrothermally stable NH_3-SCR catalyst with high selectivity at increased temperatures.[8] However, the incorporation of iron in small pore zeolites following conventional aqueous ion exchange is difficult, since the ionic diameter of hydrated Fe^{3+} ions (9 Å) is larger than the pore size found in this type of molecular sieves (3.5-4 Å).[9] For this reason, exchange is usually carried out using Fe^{2+}, which must be performed under inert atmosphere to prevent the oxidation of Fe^{2+} ions to Fe^{3+} and the formation of undesired bulky iron-species that can hardly penetrate into the zeolite pores.[8] Thus, the direct synthesis of iron-containing small pore zeolites through “one-pot” synthesis methods is desired, not

only to avoid the post-synthetic cation exchange procedures under controlled atmospheres, but also to allow a better metal distribution and stabilization within the zeolithic crystals.

Besides zeolites with the CHA framework structure, we have earlier shown that copper-containing high-silica small pore SSZ-39 zeolite (AEI structure) is an excellent NH_3-SCR catalyst,[7b,10] which in some cases even outperform copper-containing CHA in terms of activity and stability. From this finding, it would be expected that iron-containing SSZ-39 would perform comparatively well as a high temperature NH_3-SCR catalyst. However, the incorporation of iron within the AEI structure has not yet been described, probably due to the fact that this material is only achieved under very limited synthesis conditions and with low solid yields (below 40%).[11] Recently, we reported on the synthesis of high-silica SSZ-39 with improved yields (above 85%) by means of a zeolite-to-zeolite transformation procedure.[10] This method requires the use of a high silica faujasite (FAU) as the sole source of silicon and aluminum in the presence of *N,N*-dimethyl-3,5-dimethylpiperidinium (DMDMP) as the organic structure directing agent (OSDA).[10]

Herein, we describe the synthesis of iron containing SSZ-39 zeolite following two different methodologies: by aqueous post-synthetic exchange and by a "one-pot" approach. These iron-containing materials have been characterized to study the nature and stability of the iron species, and their catalytic activity has been evaluated in the NH_3-SCR reaction with an emphasis on high-temperature activity, selectivity and stability. Specifically, we have found that the iron-containing SSZ-39 material synthesized by the "one-pot" approach shows improved NH_3-SCR performance at elevated reaction temperatures (above 450ºC), after being severely aged in presence of steam, than other iron-containing zeolites.

High silica SSZ-39 for aqueous exchange was prepared by hydrothermal conversion of commercial FAU (CBV-720 with SiO_2/Al_2O_3 ratio of 21) in the presence of N,N-dimethyl-3,5-dimethylpiperidinium (DMDMP) as OSDA. The molar ratio of the synthesis mixture was SiO_2 / 0.047 Al_2O_3 / 0.2 NaOH / 0.4 OSDA / 15 H_2O, and the crystallization was carried out at 135˚C for 7 days (see experimental conditions in the Supplementary Material).[10]

Powder X-Ray diffraction (PXRD) shows that the product achieved has the AEI framework structure without the presence of other phases (see SSZ-39_1 in Figure 1). Similar to what is reported in reference [10], the solid yield was ~ 85% (inorganic basis). The chemical analysis of the sample indicates a Si/Al ratio of 9.0 and sodium content of 1.4%wt (see Table 1). For the introduction of the iron species, the sodium containing SSZ-39 was first exchanged with ammonium nitrate followed by exchange with ferrous sulfate under nitrogen atmosphere (the pH of this solution was adjusted to 3 to favor monomeric iron species in the exchange solution, see experimental conditions in the Supplementary Material). Finally, the iron-exchanged material was calcined at 550°C for 4h. ICP analysis revealed a Si/Al ratio of 8.9, an iron content of 0.9 wt% and sodium content of 0.0 wt% in the final product (see Fe-SSZ-39_1 in Table 1).

Scanning Electron Microscopy (SEM) shows that the iron-exchanged SSZ-39 sample consists of homogeneous crystals with a single rectangular morphology and an average size of ~ 300 nm (see Figure 2a). In addition, the N_2 adsorption gives a BET surface area and a micropore area of 508 and 493 m^2/g, respectively, and a micropore volume of 0.25 cm^3/g, confirming the high microporous nature of this sample (see Fe-SSZ-39_1 in Table 2).

^{27}Al MAS NMR spectroscopy was further applied to elucidate how the synthesis and post-treatment affects the state and location of aluminum in the zeolite framework. As seen in Figure 3, a single peak centered at ~ 55 ppm is observed for the as-prepared SSZ-39 material and for the iron-exchanged SSZ-39 material (see SSZ-39_1 and Fe-SSZ-39_1, respectively). These results indicate that all of the aluminum species are placed and remain in tetrahedral coordination within the AEI framework before and after the post-synthetic iron exchange.

The nature of the iron species in the exchanged was further studied by UV-Vis spectroscopy. For the exchanged Fe-SSZ-39 a single band centered at 280 nm is visible (see Fe-SSZ-39_1 in Figure 4), which has earlier been assigned to isolated Fe^{3+} ions in extra-framework positions.[6a,12] Since these extra-framework iron species have been

reported as efficient active sites for the selective catalytic reduction of NO_x with ammonia,[8,13] the catalytic activity of the exchanged sample was evaluated in the NH_3-SCR reaction.

As can be seen in Figure 5a, the exchanged Fe-SSZ-39 catalyst shows high NO conversion (almost 90%) for reaction temperatures above 500ºC, as it could be expected for an iron-based zeolithic catalyst. Its hydrothermal stability was evaluated by exposing the catalyst to steam at 600ºC for 13 hours (see experimental conditions in the Supplementary Material). The aged catalyst shows a moderate decrease in activity at higher temperatures compared to its fresh form, and NO conversion values close to 75% were obtained at reaction temperatures above 450ºC (see Fe-SSZ-39_1_HT600 in Figure 5b).

As it has been stated above, the introduction of iron species by post-synthesis procedures within small pore zeolites could be limited by diffusion. Thus, despite the good catalytic performance achieved by the iron-exchanged SSZ-39 material, it could be speculated that the catalytic behavior and the hydrothermal stability could be improved if the iron species were better distributed within the AEI crystals. The “one-pot” synthesis approach is a possible solution to improve the initial Fe dispersion as well as the aluminum distribution. Indeed, the “one-pot” synthesis approach has earlier been successful in improving the NH_3-SCR performance of different copper-containing small pore zeolites with respect to both activity as well as stability.[14]

Having the above in mind, the direct “one-pot” synthesis of iron-containing high-silica SSZ-39 zeolite was attempted by introducing ferrous nitrate into the synthesis mixture with otherwise identical components as described earlier. As the presence of iron can have an effect on crystallization, the influence of composition in the synthesis mixture was explored: OSDA/Si (0.2 and 0.4), NaOH/Si (0, 0.1, 0.2, and 0.4), and H_2O/Si (5 and 15). The Si/Fe content was fixed at 100, and the syntheses were carried out at 150ºC for 7 days under static conditions.

As summarized in Figure 6, SSZ-39 is preferentially formed when sodium is present in the synthesis gel, especially under high NaOH/Si ratios (0.2 and 0.4). The experiments

performed without sodium or under low NaOH/Si ratios (0.1) show the presence of the parent FAU zeolite in the final solids, probably because the amount of mineralizing agent in the synthesis gel is insufficient to allow partial decomposing/dissolving of the former crystalline zeolite. In contrast, when the OH^- amount is increased SSZ-39 appears, and in most cases with medium to low solid yields (< 60%), because part of the released Si and/or Al species remain in solution at high pHs. The optimum between solid yield (above 80%) and achievement of SSZ-39 material as the pure crystalline phase was found for the composition: SiO_2 / 0.047 Al_2O_3 / 0.01 Fe / 0.2 NaOH / 0.2 OSDA / 15 H_2O (see Fe-SSZ-39_2 in Figure 6).

The PXRD pattern measured on the Fe-SSZ-39_2 sample shows that only the AEI structure is obtained (see Figure 1a), without the presence of other crystalline phases. SEM microscopy furthermore shows that the sample presents a single morphology with an average crystal size of ~ 300 nm (see Figure 2b). It is worth noting that the crystal size and morphology obtained for the "one-pot" iron-containing SSZ-39 material is similar to the iron-exchanged SSZ-39 material (see Figure 2a).

The chemical analysis of the Fe-SSZ-39_2 sample indicates a Si/Al ratio of 8.0, an iron content of 1.1%wt and a sodium content of 3.3%wt (see Fe-SSZ-39_2 with sodium in Table 1). The as-prepared Fe-SSZ-39_2 material has been characterized by ^{27}Al MAS NMR and UV-Vis spectroscopy to study the coordination of the aluminum and iron species, respectively. The ^{27}Al MAS NMR spectrum shows the sole presence of aluminum in tetrahedral coordination in framework positions of the AEI structure, as revealed by the single peak centered at ~ 55 ppm (see Fe-SSZ-39_2_a.p. in Figure 3). The UV-Vis spectrum of the as-prepared Fe-SSZ-39_2 sample shows the appearance of two main absorption bands centered at 220 and 248 nm that have been associated to the presence of tetrahedrally coordinated Fe^{3+} species in framework positions.[6a,12]

To remove the sodium from the as-prepared "one-pot" Fe-SSZ-39, this sample was calcined in air at 550ºC for 4 hours, and then subjected to an ammonium exchange procedure to selectively remove the sodium cations (see experimental conditions in the

Supplementary Material). Afterwards the ammonium-exchanged "one-pot" Fe-SSZ-39 was again calcined in air at 500ºC for 4 hours to remove any residual chloride anions. From the negligible sodium content and unchanged iron content (~1%wt Fe, see Table 1), it is clear that this procedure allowed us to selectively remove sodium without changing the iron content. Furthermore, after this treatment, the aluminum species remain intact in framework positions (see the band centered at ~ 55 ppm for Fe-SSZ-39_2_calc in Figure 3). However, the UV-Vis spectrum now shows the appearance of a main band with a maximum centered at ~280 nm, which has been assigned to the presence of isolated Fe^{3+} ions in extra-framework positions.[6b] Thus, the initial tetratrahedrally coordinated iron species in framework positions observed for the "one-pot" synthesized Fe-SSZ-39, are extracted upon the exchange and calcination procedure to extra-framework positions that are generally accepted as the active site positions. [8,13]

The sodium-free "one-pot" Fe-SSZ-39 was further characterized by N_2 adsorption to compare the textural properties with that from the iron-free synthesis. The measured BET and micropore surface areas are reported in Table 2 together with the micropore volume (see Fe-SSZ-39_2 in Table 2). The values measured are higher than the ones achieved for iron-exchanged SSZ-39 (see Fe-SSZ-39_1 in Table 2), clearly showing that the introduction of iron in the synthesis mixture does not compromise the textural properties. Since both AEI materials present similar crystal sizes (see Figures 2a and 2b) and comparable iron content (see Table 1), the lower surface area and micropore volume observed for the iron-exchanged SSZ-39 material (see Fe-SSZ-39_1 in Table 1), can potentially be ascribed to an inferior metal dispersion within the AEI crystals. If this is so, the "one-pot" synthesized iron-containing SSZ-39 with a larger micropore volume and possibly a better metal distribution within the AEI crystals, should present a better catalytic activity for the NH_3-SCR compared to the iron-exchanged SSZ-39 catalyst. Indeed, the fresh sodium-free "one-pot" Fe-SSZ-39 shows an improved catalytic activity in the NH_3-SCR reaction, with NO conversion values above 95% for most of the reaction temperatures (from 350 to above 550ºC, see Figure 5a). In addition, the hydrothermal stability of the "one-pot" Fe-SSZ-39 was evaluated by submitting the catalyst to the same aging conditions as the iron-

exchanged Fe-SSZ-39 shown above (see experimental conditions in the Supplementary Material). After hydrothermal aging, a higher NO_x conversion is maintained over the "one-pot" Fe-SSZ-39 than over the exchanged Fe-SSZ-39 (see Fe-SSZ-39_2_HT600 in Figure 5b). These catalytic results, and especially those achieved for reaction temperatures above 500ºC, clearly show the potential of this type of iron-based small pore zeolites as efficient high-temperature SCR catalysts in stationary applications.

For comparison and to clearly show the benefit of SSZ-39, an iron-containing Beta zeolite was prepared following the same "one-pot" approach used for the Fe-SSZ-39. The synthesis composition was SiO_2 : 0.032 Al_2O_3 : 0.01 Fe: 0.23 TEAOH : 0.2 TEABr : 20 H_2O, and the crystallization was carried out at 140°C for 7 days (see experimental conditions in the Supplementary Material). PXRD confirms the successful formation of the Beta zeolite as the only crystalline phase obtained (see Fe-Beta_a.p. in Figure 1a). SEM microscopy also shows a single morphology with spherical particles of what is most likely agglomerates with an approximate size of ~200-300 nm (see Figure 2c). ICP analyses indicate an iron content comparable to the Fe-SSZ-39 samples, but a slightly higher Si/Al ratio (see Fe-Beta in Table 1). In a similar manner, the UV-Vis spectrum initially reveals the presence of tetrahedrally coordinated iron species in framework positions, and after calcination, they are transformed into isolated Fe^{3+} ions in extra-framework positions (see Fe-Beta_a.p. and Fe-Beta_calc in Figure 4).

The fresh Fe-Beta catalyst shows high NO conversion throughout the entire temperature range tested, similar to the ones achieved by the fresh Fe-SSZ-39 material synthesized by the same "one-pot" approach (~90% for most of the reaction temperatures, see Figure 5a). However, a severe deactivation is observed for the Fe-Beta catalyst after the hydrothermal ageing, which is more severe than for any of the Fe-SSZ-39 catalysts (see Figure 5b). These results demonstrate the benefits of using iron-containing small pore zeolites, especially those synthesized through "one-pot" methods, as efficient and hydrothermally stable high temperature NH_3-SCR catalysts.

In conclusion, the preparation of iron-containing SSZ-39 has been described following two different synthesis methodologies: a post-synthetic iron exchange and by a “one-pot” approach. These iron-containing SSZ-39 materials have been characterized, and their catalytic performance evaluated in the selective catalytic reduction of nitrogen oxides with ammonia, especially for high-temperature applications where undesired ammonia oxidation should be avoided. Both Fe-SSZ-39 catalysts show improved hydrothermal stability compared to iron-containing Beta. Moreover, the material synthesized by “one-pot” methodologies presents the highest NO conversion at high-temperature, which could be assigned to an improved dispersion of iron species compared to catalysts prepared by conventional post-synthetic exchange methods.

Acknowledgments

This work has been supported by Haldor Topsøe A/S and the Spanish Government-MINECO through “Severo Ochoa” (SEV 2012-0267), and MAT2015-71261-R is acknowledged. The European Union is also acknowledged by the SYNCATMATCH project (Grant Agreement nº 671093). N. M. thanks MINECO for economical support through pre-doctoral fellowship (BES-2013-064347). The authors thank Isabel Millet for technical support.

Figure 1: PXRD patterns of the synthesized samples in their as-prepared form (A) and after being aged at 600ºC with steam for 13 h (B)

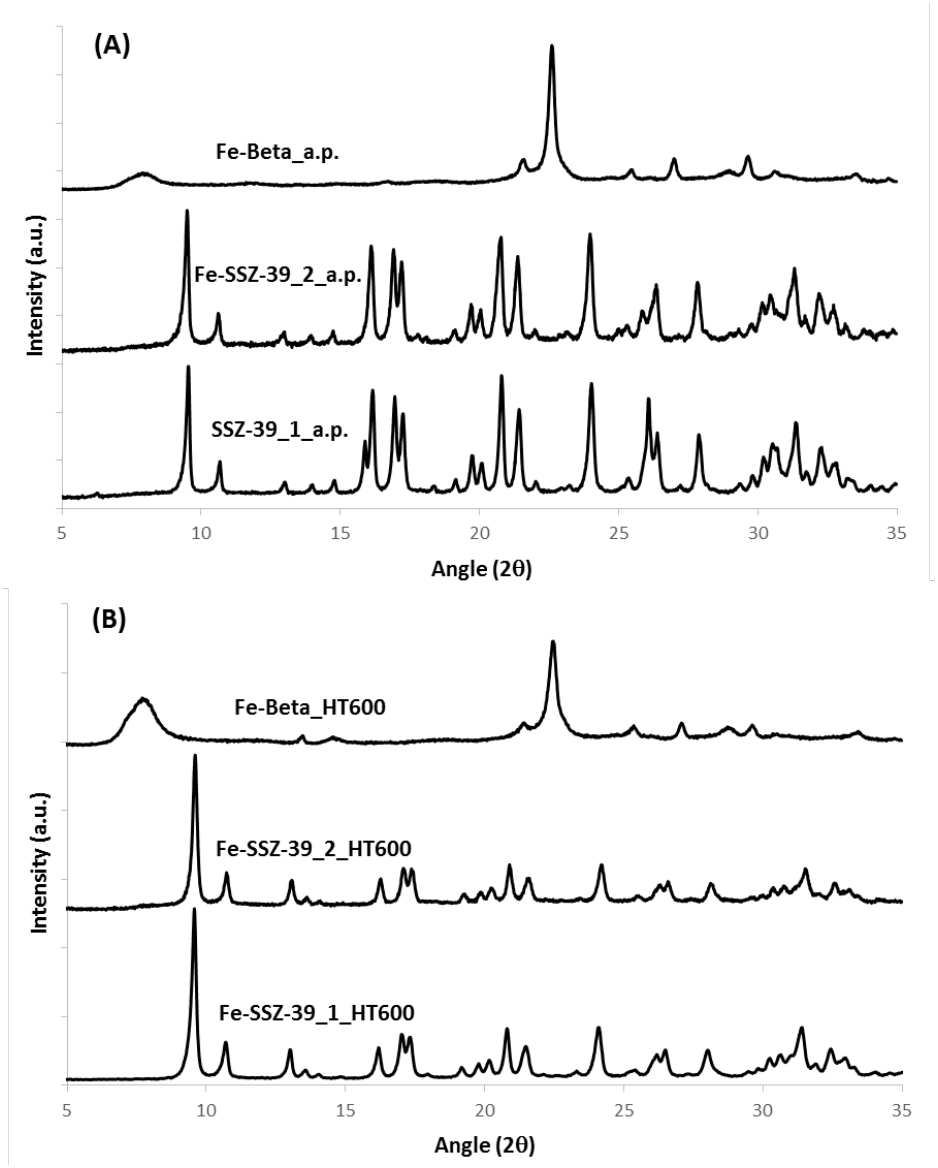

Figure 2: SEM images of the Fe-SSZ-39_1 (A), Fe-SSZ-39_2 (B) and Fe-Beta (C)

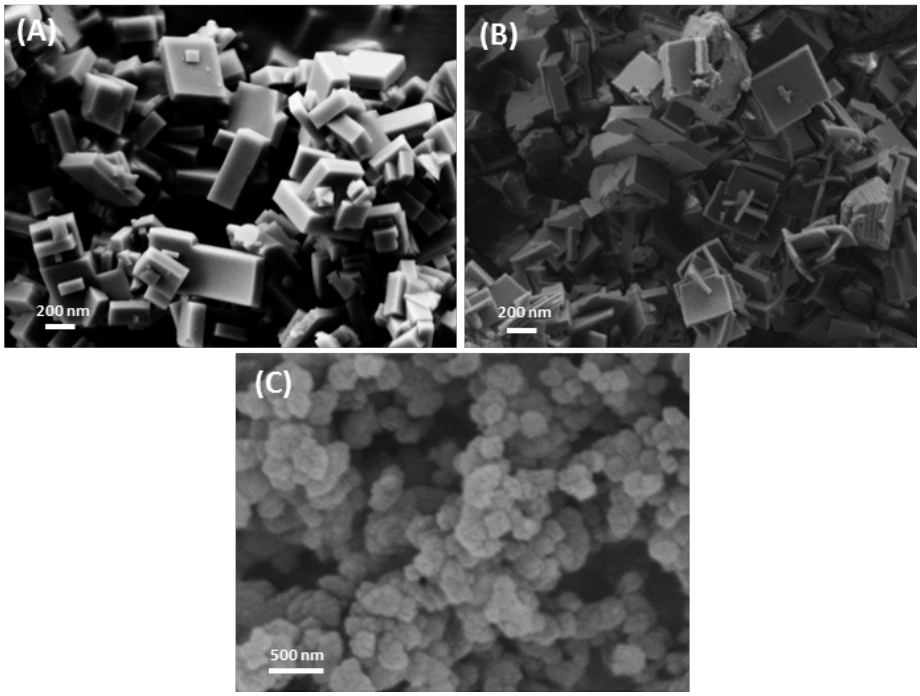

Figure 3: ^{27}Al MAS NMR spectra of the SSZ-39 samples

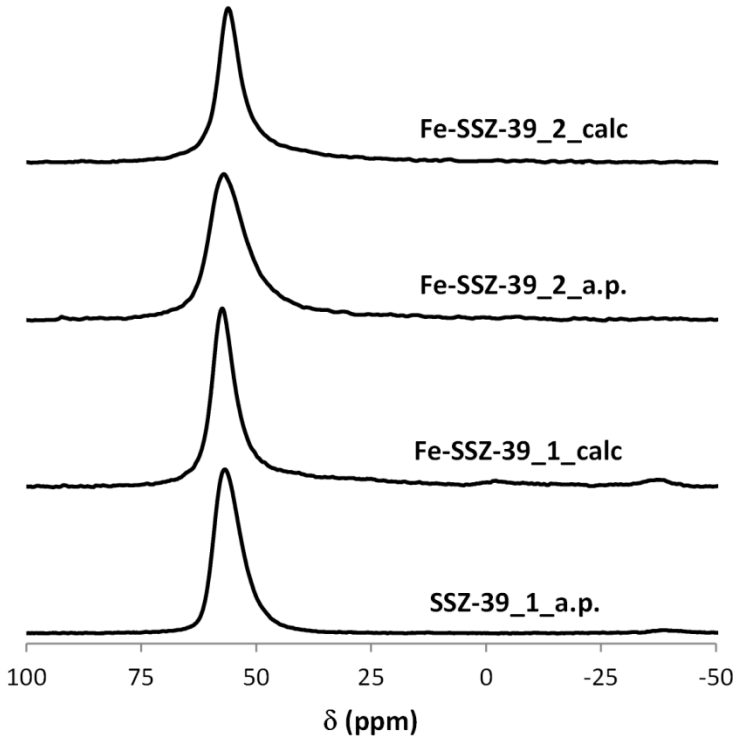

Figure 4: UV-vis spectra of the Fe-containing zeolites

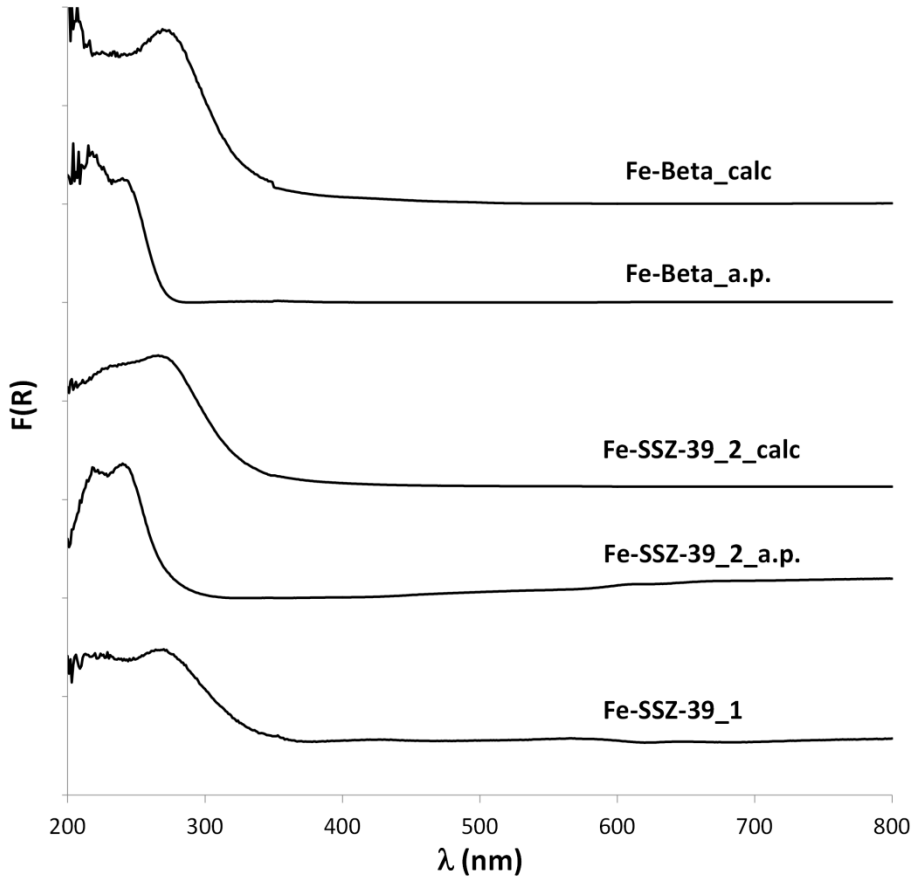

Figure 5: Catalytic activity for the NH_3-SCR of NOx reaction of Fe-AEI samples compared with Fe-Beta

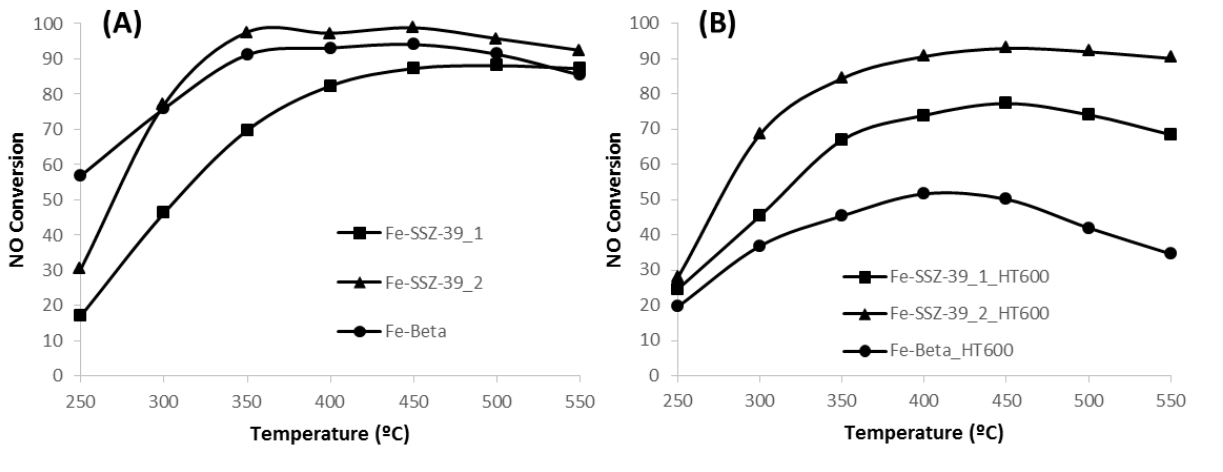

Figure 6: Phase diagram achieved for the direct synthesis of the Fe-SSZ-39 material

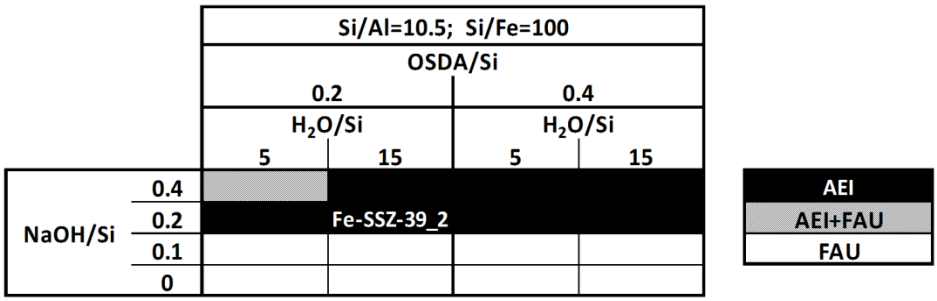

Table 1: Chemical analyses of the synthesized materials

Sample	Si/Al	%wt Na	%wt Fe
SSZ-39_1	9.0	1.4	---
Fe-SSZ-39_1	8.9	0.0	0.9
Fe-SSZ-39_2 (with Na)	8.0	3.3	1.1
Fe-SSZ-39_2 (without Na)	8.0	0.0	1.0
Fe-Beta	13.1	---	0.9

Table 2: Textural properties of the iron-containing SSZ-39 materials

Material	BET surface area (m^2/g)	Micropore area (m^2/g)	Micropore volume (cm^3/g)
Fe-SSZ-39_1	508	493	0.25
Fe-SSZ-39_2 (without Na)	614	558	0.27

SUPLEMENTARY MATERIAL

1.- Synthesis

- ***Synthesis of N, N-dimethyl-3, 5-dimethylpiperidinium (DMDMP)***

10 g of 3,5-dimethylpiperidine (C_7H_{15}, Acros Organics, 96%, cis-trans mixture) was mixed with 140 ml of methanol (CH_3OH, Scharlab, 99.9%) and with 19.5 g of potassium carbonate ($KHCO_3$, Sigma Aldrich, 99.7%). Then, 54 g of methyl iodide (CH_3I, Sigma Aldrich, 99.9%) was added dropwise under stirring. The reaction was left at room temperature under stirring for 7 days. At this point, MeOH was partially removed under vacuum, and the iodide salt was precipitated by addition of diethyl ether. The resultant iodide salt was exchanged to the hydroxide using a commercially available hydroxide ion exchange resin (Dowex SBR).

- ***Synthesis of the SSZ-39 zeolite using N, N-dimethyl-3, 5-dimethylpiperidinium hydroxide as OSDA (SSZ-39_1)***

4.48 g of a 7.4%wt aqueous solution of N,N-dimethyl-3,5-dimethylpiperidinium hydroxide was mixed with 0.34 g of a 20%wt aqueous solution of sodium hydroxide (NaOH granulated, Scharlab). The mixture was maintained under stirring 10 minutes for homogenization. Afterwards, 0.386 g of FAU zeolite (PQ Corporation, CBV-720 with SiO_2/Al_2O_3=21)[1] was added in the synthesis mixture, and maintained under stirring the required time to evaporate the excess of water until achieving the desired gel concentration. The final gel composition was SiO_2 : 0.047 Al_2O_3 : 0.4 DMDMP : 0.2 NaOH : 15 H_2O. The resultant gel was charged into a stainless steel autoclave with a Teflon liner. The crystallization was then conducted at 135°C for 7 days under static conditions. The solid product was filtered, washed with abundant amounts of water, dried at 100°C and, finally, calcined in air at 550°C for 4 h.

- ***Synthesis of Fe-containing SSZ-39 zeolite by post-synthetic ion exchange (Fe-SSZ-39_1)***

[1] The SiO_2/Al_2O_3 ratio of the USY zeolite used as precursor to overcome the SSZ-39 syntheses has been measured by ICP and EDX.

The Na-containing SSZ-39_1 material was first exchanged with a 0.1 M solution of ammonium nitrate (NH_4NO_3, Fluka, 99 wt%) at 80°C. Afterwards, 0.1 g of ammonium-exchanged SSZ-39 zeolite was dispersed in 10 ml of deionized water with pH adjusted to 3 using 0.1 M HNO_3. The suspension was heated to 80°C under nitrogen atmosphere, and then, 0.0002 moles of $FeSO_4.7H_2O$ was added, maintaining the resultant suspension under stirring for 1 h at 80°C. Finally, the sample was filtered, washed and calcined at 550°C for 4h.

- ***Direct synthesis of the Fe-containing SSZ-39 zeolite [Fe-SSZ-39_2 (with Na)]***

1.98 g of a 7.0%wt aqueous solution of N,N-dimethyl-3,5-dimethylpiperidinium hydroxide was mixed with 0.24 g of a 20%wt aqueous solution of sodium hydroxide (NaOH granulated, Scharlab). The mixture was maintained under stirring 10 minutes for homogenization. Afterwards, 0.303 g of FAU zeolite (Zeolyst CBV-720 with SiO_2/Al_2O_3=21)[1] was added in the synthesis mixture. Finally, 0.11 g of a 20%wt aqueous solution of iron (III) nitrate [$Fe(NO_3)_3$, Sigma Aldrich, 98%] was added, and the synthesis mixture was maintained under stirring the required time to evaporate the excess of water until achieving the desired gel concentration. The final gel composition was SiO_2 : 0.047 Al_2O_3 : 0.01 Fe: 0.2 DMDMP : 0.2 NaOH : 15 H_2O. The resultant gel was charged into a stainless steel autoclave with a Teflon liner. The crystallization was then conducted at 140°C for 7 days under static conditions. The solid product was filtered, washed with abundant water, and dried at 100°C. Finally, the as-prepared solid was calcined in air at 550°C for 4 h. The solid yield achieved was above 85% (without taking into account the organic moieties).

- ***Removal of Na from the Fe-containing SSZ-39 material by ammonium-exchange procedure [Fe-SSZ-39_2 (without Na)]***

200 mg of the calcined Fe-SSZ-39_2 material was mixed with 2 ml of a 1 M aqueous solution of ammonium chloride (Sigma-Aldrich, 98%wt), and the mixture was maintained under stirring at 80°C for 5 h. The solid product was filtered, washed with abundant water, and dried at 100°C. Finally, the solid was calcined in air at 500°C for 4 h.

- ***Direct synthesis of the Fe-containing Beta structure (Fe-Beta)***

0.40 g of a 35%wt aqueous solution of tetraethylammonium hydroxide (TEAOH, Sigma-Aldrich) was mixed with 0.34 g of a 50%wt aqueous solution of tetraethylammonium bromide (TEABr, Sigma-Aldrich). Then, 0.60 g of a colloidal suspension of silica in water (40%wt, LUDOX-AS, Sigma-Aldrich) and 18 mg of alumina (75%wt, Condea) were added, and the resultant mixture maintained under stirring for 15 minutes. Finally, 0.33 g of a 5%wt aqueous solution of iron (III) nitrate [$Fe(NO_3)_3$, Sigma Aldrich, 98%] was added, and the synthesis mixture was maintained under stirring the required time to evaporate the excess of water until achieving the desired gel concentration. The final gel composition was SiO_2 : 0.032 Al_2O_3 : 0.01 Fe: 0.23 TEAOH : 0.2 TEABr : 20 H_2O. The resultant gel was charged into a stainless steel autoclave with a Teflon liner. The crystallization was then conducted at 140°C for 7 days under static conditions. The solid product was filtered, washed with abundant water, and dried and finally calcined in air at 550°C for 4 h.

- ***Accelerated hydrothermal ageing treatment of the iron-containing catalysts***

The iron-containing catalysts were treated in a gas mixture containing 10% H_2O, 10% O_2 and N_2 for 13 hours at 600°C, and afterwards, their catalytic performance was evaluated again.

2.- Characterization

The crystallinity of the samples was measured by powder X-ray diffraction (PXRD) with a Panalytical CUBIX diffract meter with monochromatic $CuK_{\alpha 1,2}$ radiation (λ=1.5406, 1.5444 Å; $K\alpha_2$ / $K\alpha_1$ intensity ratio=0.5).

The morphology and particle size of the zeolites were characterized by Scanning Electron Microscope (SEM, JEOL JSM-6300).

The MAS NMR spectra were recorded with a Bruker AV400 spectrometer. Solid state ^{27}Al MAS NMR spectra were recorded at 104.218 MHz with a spinning rate of 10 kHz at a 90°

pulse length of 0.5 μs with 1 s repetition time. ^{27}Al chemical shifts were referred to $[Al(H_2O)_6]^{3+}$.

Chemical composition was determined by inductively coupled plasma atomic absorption spectroscopy (ICP-OES) using a Varian 715-ES.

The BET surface area, micropore volume and pore volume distribution were measured by N_2 adsorption in a Micromeritics ASAP2000.

UV–Vis spectra were obtained with a Perkin–Elmer (Lambda 19) spectrometer equipped with an integrating sphere with $BaSO_4$ as reference.

3.- Catalytic test

The activity of selected samples was evaluated in the catalytic reduction of NOx using NH_3 in a fixed bed, quartz tubular reactor of 1.2 cm of diameter and 20 cm of length. The catalyst was tested using 40 mg with a sieve fraction of 0.25-0.42 mm. The catalyst was introduced in the reactor, heated up to 550°C in a 300 ml/min flow of nitrogen and maintained at this temperature for one hour. Afterwards, 50 ppm NO, 60 ppm NH_3, 10 $\%O_2$ and 10% H_2O was admitted over the catalyst while maintaining a flow of 300 ml/min. The temperature was then decreased stepwise between 550 and 250°C. The conversion of NO was measured under steady state conversion at each temperature using a chemiluminiscence detector (Thermo 62C).

References

[1] (a) B. Guan, R. Zhan, H. Lin, Z. Huang, Appl. Therm. Eng., 2014, 66, 395; (b) M. V. Twigg, Appl. Catal. B, 2007, 70, 2.
[2] (a) C. Ciardelli, I. Nova, E. Tronconi, D. Chatterjee, B. Bandl-Konrad, M. Weibel, B. Krutzsch, Appl. Catal. B, 2007, 70, 80; (b) I. Nova, C. Ciardelli, E. Tronconi, D. Chatterjee, B. Bandl-Konrad, Catal. Today, 2006, 114, 3.
[3] (a) S. Brandenberger, O. Kröcher, A. Tissler, R. Althoff, Catal. Rev. Sci. Eng., 2008, 50, 492; (b) M. Iwamoto, H. Furukawa, Y. Mine, F. Uemura, S.I. Mikuriya, S. Kagawa, J. Chem. Soc., Chem. Commun., 1986, 1272.
[4] (a) D. W. Fickel, E. D'Addio, J. A. Lauterbach, R. F. Lobo, Appl. Catal. B, 2011, 102, 441; (b) M. Moliner, C. Martínez, A. Corma, Chem. Mater. 2014, 26, 246; (c) J. H. Kwak, R. G. Tonkyn, D. H. Kim, J. Szanyi and C. H. F. Peden, J. Catal., 2010, 275.
[5] (a) M. Colombo, I. Nova, E. Tronconi, Catal. Today, 2010, 151, 223; P. S. Metkar, M. P. Harold, V. Balakotaiah, Appl. Catal. B, 2012, 111–112, 67.
[6] (a) J. Perez-Ramirez, J. C. Groen, A. Brückner, M. S. Kumar, U. Bentrup, M. N. Debbagh, L. A. Villaescusa, J. Catal., 2005, 232, 318; (b) M. Iwasaki, H. Shinjoh, Chem. Commun., 2011, 47, 3966; (c) R. Nedyalkova, S. Shwan, M. Skoglundh, L. Olsson, Appl. Catal. B, 2013, 138-139, 373; (d) P. Boron, L. Chmierlarz, J. Gurgul, K. Latka, B. Gil, B. Marszalek, S. Dzwigaj, Micropor. Mesopor. Mater., 2015, 203, 73.
[7] (a) I. Bull, U. Muller, *US2010/0310440A1*, 2010; (b) M. Moliner, C. Franch, E. Palomares, M. Grill, A. Corma, Chem.Commun., 2012, 48, 8264.
[8] F. Gao, M. Kollar, R. K. Kukkadapu, N. M. Washton, Y. Wang, J. Szanyi, C. H. F. Peden, Appl. Catal. B., 2015, 164, 407.
[9] J. Kielland, J. Am. Chem. Soc., 1937, 59, 1675.
[10] N. Martin, C. R. Boruntea, M. Moliner, A. Corma, Chem. Commun., 2015, 51, 11030.
[11] (a) S. I. Zones, Y. Nakagawa, S. T. Evans and G. S. Lee, U.S. Patent, 5,958,370, 1999; (b) P. Wagner, Y. Nakagawa, G. S. Lee, M. E. Davis, S. Elomari, R. C. Medrud, S. I. Zones, J. Am. Chem. Soc., 2000, 122, 263.
[12] S. Bordiga, R. Buzzoni, F. Geobaldo, C. Lamberti, E. Giamello, A. Zecchina, G. Leofanti, G. Petrini, G. Tozzola, G. Vlaic, J. Catal., 1996, 158, 486.
[13] S. Brandenberger, O. Kröcher, A. Tissler, R. Althoff, Appl. Catal. B, 2010, 95, 348.
[14] (a) R. Martínez-Franco, M. Moliner, C. Franch, A. Kustov, A. Corma, Appl. Catal. B, 2012, 127, 273; (b) R. Martínez-Franco, M. Moliner, P. Concepcion, J. R. Thogersen, A. Corma, J. Catal., 2014, 314, 73; (c) R. Martínez-Franco, M. Moliner, A. Corma, J. Catal., 2014, 319, 36.